Fractal geometry of the fatigue fracture surface of the ZTA composites

M V Korobenkov[1], T A Kiseleva[2]

[1]Immanuel Kant Baltic Federal University, Kaliningrad, Russia
[2]National Research Tomsk State University, Tomsk, Russia

E-mail: MKorobenkov@kantiana.ru

Abstract. A fracture surface of the ceramic composite Al_2O_3 - ZrO_2 at three-point bending during fatigue loading has been studied by scanning electron microscope. The bending strength and flexural modulus are derived under static conditions at a loading rate of 3 mm/min. The fatigue strength and fatigue limit are investigated at a frequency of 4 Hz in three stress ranges: 0.9, 0.8 and 0.7 of the average maximum static bending strengths. The surface fractal dimensions D_f is determined using triangulation method. It was shown that the surface relief can be characterized by fractal relief in the local approximation. The fractal dimensionality of the studied surface changes in the relatively narrow limits D_f = 2.653 - 2.742, for ceramic samples sintered at 1650 ℃, and highly dependent on the number of cycles. The ceramic samples sintered at 1400 ℃ showed low resistance to fatigue loads with the fractal dimensionality D_f = 2.710 - 2.781, which are independent of the number of cycles.

1. Introduction

It is known the most significant factor affecting ceramic mechanical properties is the porosity. On the other hand, the effectiveness of such materials is mostly determined by the parameters of the pore structure [1-3]. Among the variety of structural ceramic materials, investigations of partially stabilized zirconia-based ceramics are of the prime interest due to a comprehensive impact of porosity, grain structure, and phase composition on their mechanical behavior. Nowadays, a lot of research are devoted to the relationship between the internal structure of zirconia-based ceramics, metal-matrix composites, functionally graded materials and their mechanical properties, like compressive strength, bending strength, fracture toughness, impact resistance and microhardness [4-6]. In [7] functionally graded materials were used to increase the impact resistance and survivability target under impact loading. However, only a little bit is known about the fatigue behaviour of porous ceramic materials. Although there is a relatively large number of studies on the fatigue behaviour of advanced ceramics, most of them have been mainly concerned about demonstrating and explaining the mechanical side of cyclic fatigue in these materials [8]. On the other hand, only a few studies have been focused on the description and interpretation of the influence of microstructural parameters on the fatigue behaviour of toughened ceramics. One of the methods for determining the structural level of nucleation of fatigue fracture can be a fractal geometry of the fracture surface.

Assuming that the investigated fracture surface is a fractal object, we can use general ideas about fractal objects to analyze it. When carrying out a fractal analysis of images, their features must be taken into account. It is known that the surfaces of solids can be characterized by different values of

the fractal dimension for different ranges of the measuring scale. Such fractal objects are called self-affine in contrast to self-similar objects, which are characterized by one fractal dimension. The fractal dimension values founded in this way correspond to the so-called local limit. At the same time, studying the surface morphology with high resolution in order to reliably determine the fractal dimension, when the scanning step is comparable with the size of the irregularities is necessary [9]. Due to the specifics of the implementation of SEM images in our studies, this becomes possible with a significant reduction in the scanned area. As you deviate from this condition, the determined fractal dimension of the surface decreases and tends to the "usual" (topological) dimension. It should be added that the surfaces of real physical objects are only statistically self-affine. The magnitude of the fractal dimension may vary in different parts of the surface. We can only talk about the average value of the fractal dimension, which obtained by averaging the fractal dimensions calculated for different parts of the surface. Fractal parameters of fracture surfaces were determined by the method of triangulation [10, 11] from images from a VEGA3 TESCAN electron scanning microscope at different scale levels.

The purpose of this work is the study of the fractal geometry of the fracture surface of the ZTA composites obtained under fatigue three-point bending test.

2. Materials and experimental

The green compact of the ceramic composites was obtained by forming blanks in molds prismatic samples of the powder mixture with a ratio of 20 % (ZrO_2 - (3 % MgO)) – 80 % (α - Al_2O_3). The green compact was sintered at temperatures of 1400 °C, 1500 °C and 1650 °C with high-temperature exposure for one hour.

The porosity of the samples was measured by a hydrostatic method in distilled water according to the following equation:

$$\theta = \frac{\rho_{th} - \rho_e}{\rho_{th}} * 100\%, \tag{1}$$

where ρ_{th} is the theoretical density, ρ_e - experimental density of the material.

The experimental density of the sample id determined according to the following equation:

$$\rho_e = \frac{m_1}{m_1 - m_2} * \rho_l, \tag{2}$$

where m_1 is the mass of the sample suspended in air, g; m_2 is the mass of the sample, varnished and suspended in water, g; ρ_l is the density of the liquid, g/mm³.

The physical and mechanical properties of the specimens were investigated by the three-point bending technique, using the Instron ElectroPuls E1000 test system. The span between two supports holder was 30 mm for the samples with a porosity of 6.5 % and 11 %, and 36 mm for the samples with a porosity of 21 %.

The value of tensile strength σ_{ben} and flexural modulus E_{ben} of ceramic composites was determined as a strain rate of 0.3 mm/min using five samples of the same series according to the following equation [12]:

$$\sigma_{ben} = \frac{3Pl}{2bh^2}, E_{ben} = \frac{Pl^3}{4fbh^3}, \tag{3}$$

where P is the load at the fracture, which was determined during the test sample, N; l is the support span, mm; b is the width of the sample, mm; h is the thickness of the sample, mm; f is the specimen deflection, mm.

Loading conditions were assigned in terms of unipolar loading waves from 8 N with double amplitude D of the cycle corresponding to three stress ranges: 0.9, 0.8 and 0.7 of the average maximum static bending strengths at a frequency of $v = 4$ Hz for measuring the fatigue life. The parameters of the fatigue tests were chosen in a way to provide the required stiffness of the testing system with reasonable accuracy in the fulfilment of the specified conditions in the loading cycle.

The structure of the fracture surface of the ceramics was studied by using scanning electron microscope TescanVega 3. Scan modes were selected by the structural features of the samples.

The fractal analysis of the fatigue surface relief of the ceramic composites was performed by the calculation program of the fractal dimensionalities D_f of the surface region based on the measurement of their area by the triangulation method. The triangulation method is based on measurement of the actual area values of the surface S_{fact} depending on the measuring scale l_i, or the effective parameters δ_i. According to [13-15], each value of the parameter $\delta_i = 1/i$ ($i=1, 2, 3, …, N$) for the fractal surface correlates with its definite value of the area of the i_{th} pre-fractal of this surface:

$$S_{fact,i} = S_0 \delta_i^{2-D_f}. \tag{4}$$

The D_f value was determined from the slope of the linear region of the dependence $\ln (S_{fact, i})$ on $\ln (\delta_i)$.

The surface irregularity $\Delta h\,(x, y)$ was determined as the distance between the measured $h\,(x, y)$ grey value and the minimum $h\,(x, y) = h_{min}$. The minimum value for the studied region was taken as zero, $h_{min} = 0$:

$$\Delta h(x, y) = h(x, y) - h_{min}. \tag{5}$$

The mean surface roughness R_a was determined as the mean deviation from the mean grey value of the irregularity height $\overline{\Delta h}$:

$$R_a = \frac{1}{N_i} \sum_i \left(\Delta h_i - \overline{\Delta h}\right), \text{where } \overline{\Delta h} = \frac{1}{N_i} \sum_i \overline{\Delta h}. \tag{6}$$

The treatment parameters were the L, $\overline{\Delta h}$, D_f, R_a, and S_{fact} values for different areas.

3. Results and discussion

Figure 1 shows the results of measurement for the fractal dimension of the fracture surface (600000 cycles of load) of the ceramic composite sintered at 1400 °C under study by the triangulation method, profile of the transverse cross-section of the relief and the dependence of $\ln (S_{fact}/S_0)$ on $\ln (1/\delta)$ for calculating the fractal dimension D_f.

The research results showed the fractal dimension corresponds to a value of 2.781 for a local approximation of 100 micrometres and decreases to 2.75 in a local approximation of 10 micrometres for samples with a porosity of 21%. The values of the fractal dimension are independent of the number of cycles until the destruction of the samples.

Figure 2 shows the results of measurement for the fractal dimension of the fracture surface (100000 cycles of load) of ceramic composite sintered at 1500 °C under study by the triangulation method, profile of the transverse cross-section of the relief and the dependence of $\ln (S_{fact}/S_0)$ on $\ln (1/\delta)$ for calculating the fractal dimension D_f.

The research results showed the fractal dimension corresponds to a value of 2.756 for a local approximation of 100 micrometres and decreases to 2.718 in a local approximation of 10 micrometres for samples that did not withstand more than 100000 cycles before fracturing for samples with a porosity of 11 %. The fractal dimension is 2.88 to a local approximation of 100 micrometres and decreases to 2.68 for the local approximation of 10 micrometres for samples have failed before 1000 test cycles.

Figure 3 shows the results of measurement for the fractal dimension of the fracture surface (650000 cycles of load) of ceramic composite sintered at 1650 °C under study by the triangulation method, profile of the transverse cross-section of the relief and the dependence of $\ln (S_{fact}/S_0)$ on $\ln (1/\delta)$ for calculating the fractal dimension D_f.

The research results showed that the fractal dimension corresponds to a value of 2.85 for a local approximation of 100 micrometres for samples that break down to 100000 cycles and decrease to 2.64 in a local approximation of 10 micrometres for samples with a porosity of 6.5 %. The fractal dimension corresponds to a value of 2.742 for a local approximation of 100 micrometres for samples that break after 500,000 cycles and decreases to 2.653 in a local approximation of 10 micrometres. The values of the fractal dimension for samples with a porosity of 11 % and 6.5 % are dependent on the number of cycles until the destruction.

On figure 3 two linear regions are noteworthy in the dependencies $\ln (S_{fact}/S_0)$ on $\ln (1/\delta)$. The linear region with D_f=2.273 corresponding to a larger δ has the fractal dimension closer to 2; the linear

region with $D_f = 2.742$ corresponding to a smaller δ has a larger slope, hence, a larger dimension. We can see that, as the scanned area decreases, the approximate line length decreases with a simultaneous increasing in its slope. Simultaneously, the 2nd approximate line length increases, and its slope also slightly increases. Studies of areas with scale of 5 μm showed that the knee in the dependence of ln (S_{fact}/S_0) on ln (1/δ) almost disappears, and this dependence can be described by a single linear dependence with $D_f \geq 2.65$. The slight variation in D_f for various areas in the right approximate regions reflects the statistically self-affine behavior of the fracture surface.
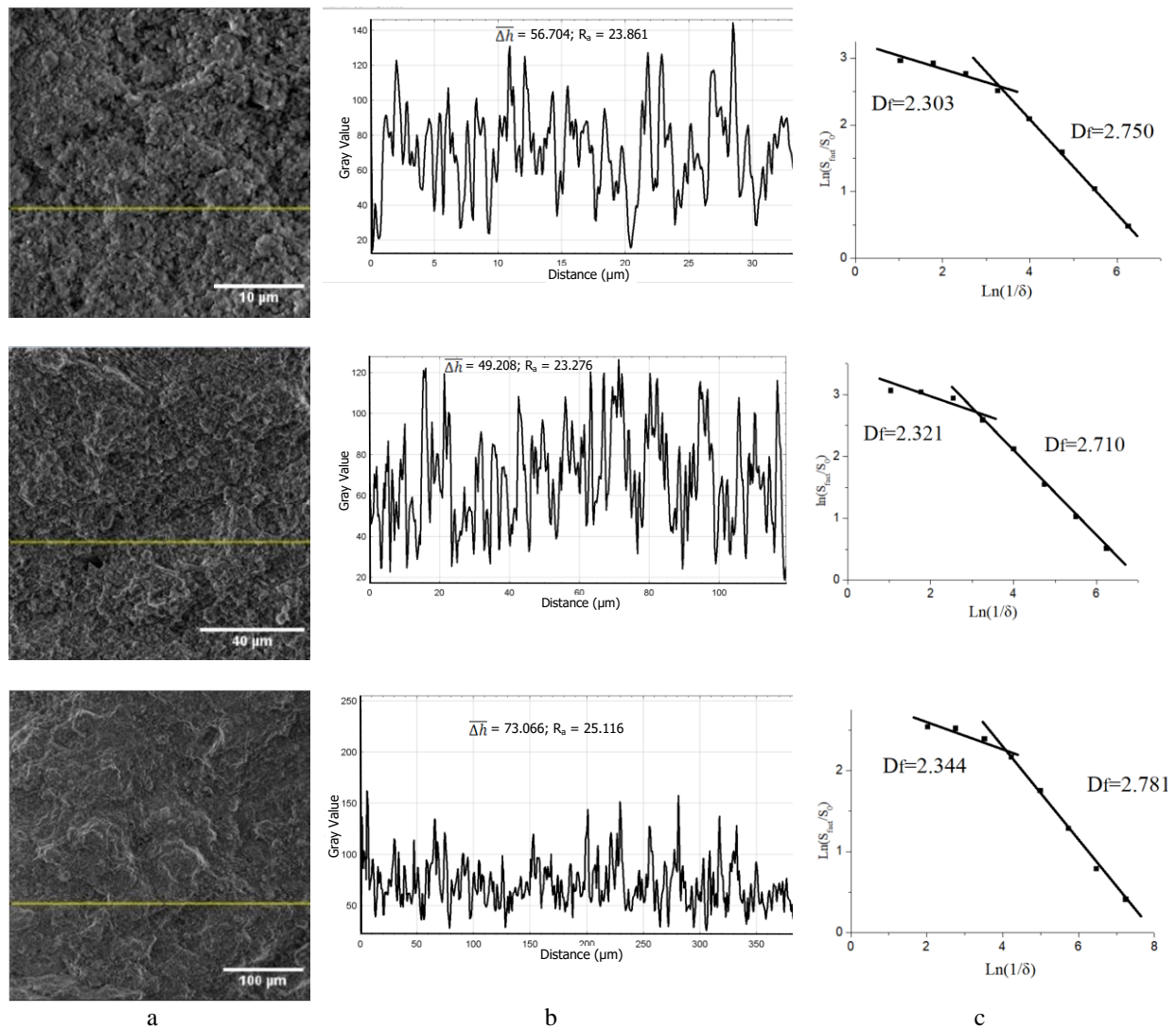

Figure 1. The SEM images of fracture fatigue surface (a), profiles of the transverse cross-section of the relief Δh (y) (b) and the dependences of ln (S_{fact}/S_0) on ln (δ) for determining the fractal dimensions by triangular method (c) for ZTA composite with a porosity 21 %

The fracture surface is nonfractal, i.e., flat, for the large δ (exceeding the particle size). In other hands, its fractal dimension is equal to the topological one, $D_f \approx 2$. On the contrary, the linear region with small δ corresponds to the fractal surface. The value corresponding to the knee in the dependences of ln (S_{fact}/S_0) on ln (1/δ) can be interpreted as a certain upper limit bound for determining the fractal dimension. The region of smaller δ, where the surface behaves as a fractal object, corresponds to the so-called local approach (limit) in the definition of the fractal dimension; whereas, for the region of

larger δ, we can formally speak about a global approximation (limit) in the definition of the surface dimension. As noted above, this case corresponds to the surface dimension closer to 2, i.e., the topological dimension. The local transition in determining the fractal surface size corresponds to the approximation of the size of the grain structure.
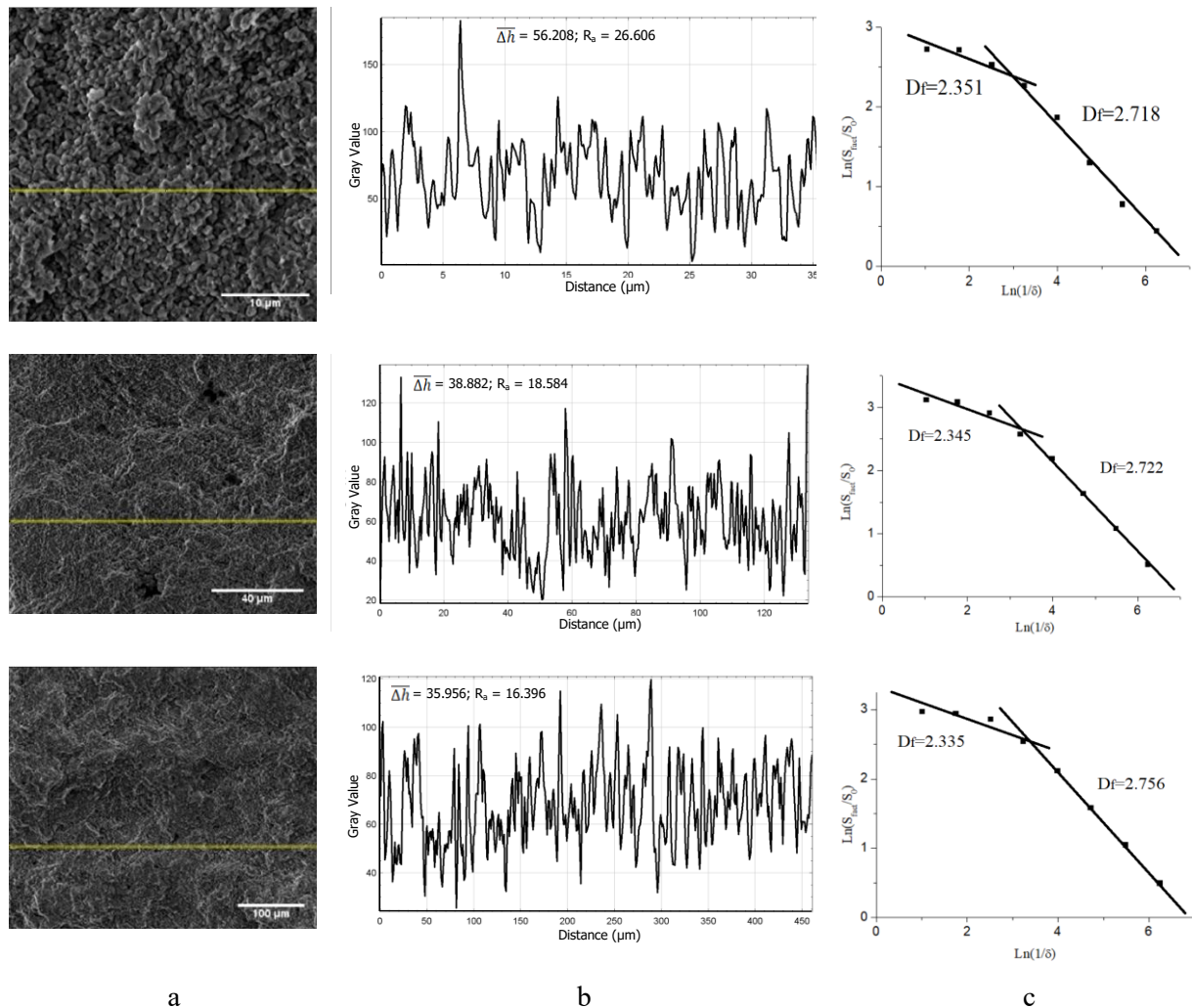

         a   b   c

Figure 2. The SEM images of fracture fatigue surface (a), profiles of the transverse cross-section of the relief Δh (y) (b) and the dependences of $\ln (S_{fact}/S_0)$ on $\ln (\delta)$ for determining the fractal dimensions by a triangular method (c) for ZTA composite with a porosity 11 %

SEM image analysis showed the propagation of cracks only along grain boundaries. Such grain boundary weakness was explained by microcracking which resulted from the localized deposition of eutectoid decomposition product of them. The cracks in the boundary layer of the grains accumulate and pass into fatigue micro-cracks and then into meso-cracks.

The experimental relationship between flexural modulus and specimen deflection is shown in figure 4a. Experimental data point for the fatigue bending test is presented in figure 4b. The fatigue limits for specimens with pores increased with decreasing pore content, the same dependence is observed with static tests.
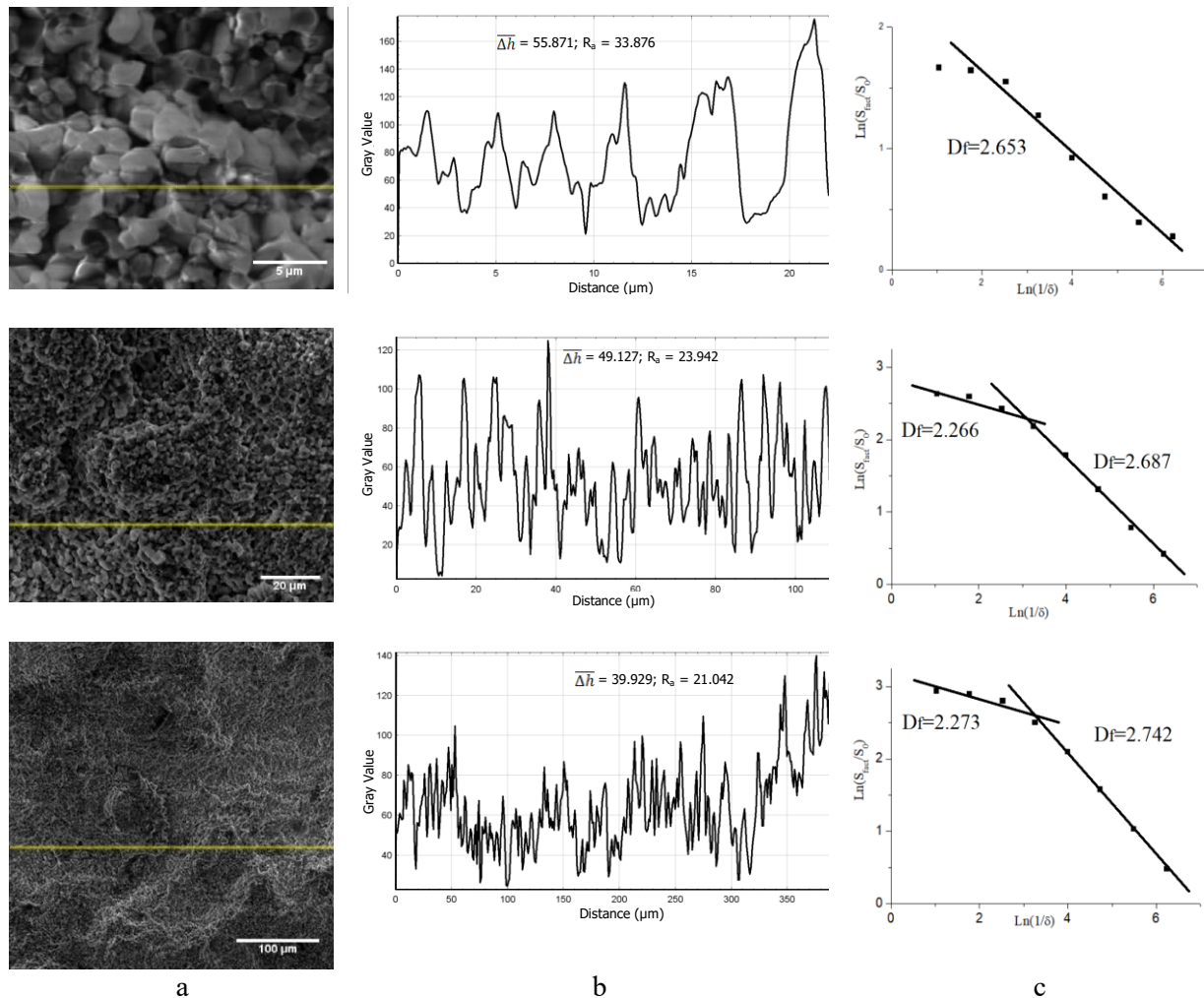
Figure 3. The SEM images of fracture fatigue surface (a), profiles of the transverse cross-section of the relief Δh (y) (b) and the dependences of ln (S_{fact}/S_0) on ln(δ) for determining the fractal dimensions by triangular method (c) for ZTA composite with a porosity 6.5 %
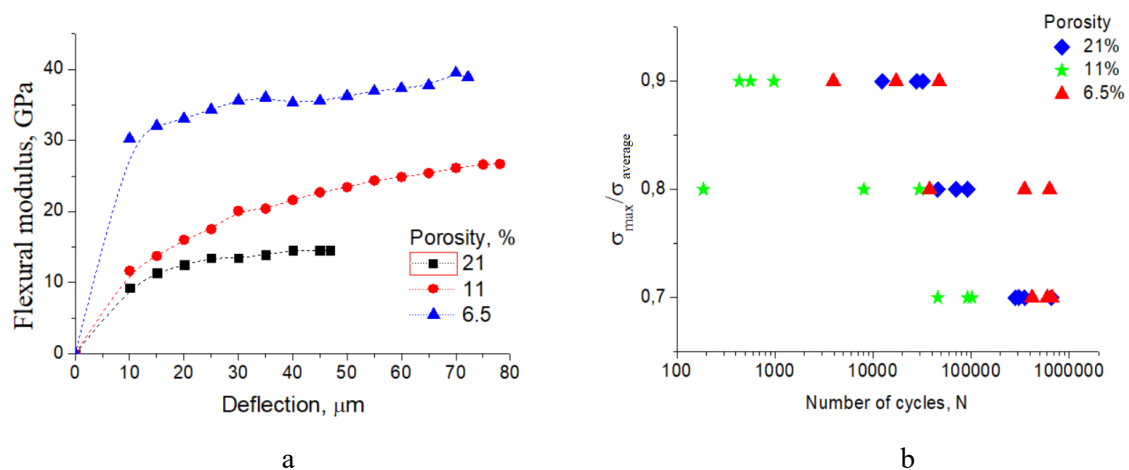

Figure 4. Experimental relationship between flexural modulus and specimen deflection (a) and fatigue bending test results (b) for ZTA composites

4. Conclusions

The bending strength and flexural modulus of the ZTA composite with different pore structure were evaluated by a three-point bending test. The fatigue strength and fatigue limit under dynamic loading conditions are investigated. The fatigue limits for specimens with pores increased with decreasing pore content, the same dependence is observed in static tests. SEM image analysis showed the propagation of cracks only along grain boundaries. Such grain boundary weakness was explained by microcracking which resulted from the localized deposition of eutectoid decomposition product of them.

Studies have shown that the fracture surface is nonfractal, i.e., flat, for the large δ (exceeding the particle size). The slight variation in D_f for various areas in the right approximate regions reflects the statistically self-affine behavior of the fracture surface. The value corresponding to the knee in the dependences of $\ln(S_{fact}/S_0)$ on $\ln(1/\delta)$ can be interpreted as a certain upper limit bound for determining the fractal dimension. The region of smaller δ, where the surface behaves as a fractal object, corresponds to the so-called local approach (limit) in the definition of the fractal dimension; whereas, for the region of larger δ, we can formally speak about a global approximation (limit) in the definition of the surface dimension.

Thus, as a result of the conducted studies, it can be concluded that fracture surfaces lead to the formation of self-affine surface relief, characterized by the local limit by a set of fractal dimension values. The range of these values for the studied range of values of the measuring scale is small, and in principle, for the entire range of δ values (where the local approximation can be used), one can introduce the statistical value of the fractal dimension of the surface.

Notification

ZTA - Zirconia toughened alumina

θ - porosity

ρ_{th} - theoretical density of the material

ρ_e - experimental density of the material

m_1 - mass of the sample suspended in air

m_2 - mass of the sample, varnished and suspended in water

ρ_l - density of the liquid

σ_{ben} - tensile strength

E_{ben} - flexural modulus

P - load at the fracture

l - the support span

b - width of the prismatic sample

h - thickness of the prismatic sample

f - specimen deflection

D - double amplitude

v – frequency of load

D_f - fractal dimension

S_{fact} - actual area values of the surface

l_i - measuring scale

δ_i - effective parameter of the measuring scale

S_0 - topological area of the studied surface region

$\Delta h\,(x, y)$ - surface irregularity

$h\,(x, y)$ - grey value for the SEM image

$h_{\min}$ – minimum of the gray value for the SEM image

R_a - mean surface roughness

$\overline{\Delta h}$ - mean grey value of the irregularity height

L – linear size of the measured area

References

[1] Korobenkov M V and Kulkov S N 2017 *AIP Conf. Proc.* **1882** 020035

[2] Fischer J, Stawarczyk B and Hammerle C H F 2008 *J. Dentistry* **36(5)** pp 316-321

[3] Levkov R V, Pigaleva N V, Korobenkov M V and Kulkov S N 2018 *J. Phys.: Conf. Ser.* **1045** 012027

[4] Korobenkov M V, Kulkov S N, Naymark O B, Khorechko U V and Ruchina A V 2016 *IOP Conf. Ser.: Mater. Sci. Eng.* **112** 012044

[5] Kozulin A A et al 2012 *Izv. Vissh. Uchebn. Zaved. Fizika* **55(7/2)** pp 81-85

[6] Korobenkov M, Kulkov S, Leitsin V and Tovpinets A 2018 *MATEC Web Conf.* **243** 00025

[7] Orlov M Yu, Orlov Yu N, Glazyrin V P and Orlova Yu N *EPL Web of Conf.* **183** 01049

[8] Souza R C, Dos Santos C, Barboza M J R, De Araujo Bicalho L, Baptista C A R P and Elias C N 2014 *J. Mater. Res. Tech.* **39(1)** pp 48-54

[9] Family F and Vicsek T 1991 *Dynamic of fractal surfaces* (Singapore: World Sci.)

[10] Ankudinov A V, Evtikheev V P, Ladutenko K S et al. 2006 *Semiconductors* **40** pp 982-989

[11] Torkhov N A, Bozhkov V G, Ivonin I V and Novikov V A 2009 *Semiconductors* **43** pp 33-41

[12] Kozulin A A, Narikovich A S, Kulkov S N, Leitsin V N and Kulkov S S 2016 *AIP Conf. Proc.* **1760** 020036

[13] Feder J 1988 *Fractals* (New York: Plenum Press)

[14] Mandelbot B B 2002 *Fractal geometry of the Nature* (Moscow: Inst. Komp. Issled)

[15] Torkhov N A 2010 *J. Synch. Investig.* **4** pp. 45-58